CHALMERS

DEVELOPMENT AND IMPLEMENTATION OF A RAPID DEPLOYMENT SYSTEM FOR VOLCANIC GAS EMISSION MONITORING

Master of Science Thesis in the Master Degree Programme, Radio and Space Science

ALEXANDER VLADIMIR CONDE

Department of Earth and Space Science

CHALMERS UNIVERSITY OF TECHNOLOGY

Göteborg, Sweden, 2010

ABSTRACT

Volcanic eruptions are one of the most impressing geophysical phenomenons. There are more than 500 active volcanoes around the world. Across the time, large populations have been benefitted with better agriculture in volcanic soils due to natural fertilization. On the other hand active volcanoes close to populated areas represent a natural hazard.

A constant monitoring of the volcano activity reduces the risk in potentially affected areas; for the last decades this has motivated the development of different volcanic surveillance techniques: seismicity, geodesy and geochemistry. In particular, monitoring volcanic gas emissions has acquired major importance as an indicator of changes in the volcanic activity. Among different ways to do that, optical remote sensing has been successfully applied as an efficient and safe method to quantify volcanic gas emissions.

This thesis presents the design of a network of optical remote sensing instruments for monitoring volcanic gas emissions. The monitoring technique is based on DOAS (Differential Optical Absorption Spectroscopy). The system compiles measuring techniques previously developed by the Optical Remote Sensing Group of Chalmers in a deployable way, taking advantage of recent hardware development.

This network was tested in a real application, making SO_2 flux measurements continuously during 3 months at Télica volcano (Nicaragua), and transmitting the data by a satellite link to a server located at Chalmers.

A shorter experiment was also conducted at Popocatépetl volcano (México) where the portability of the systems allows us to keep tracking the wide variations of the volcanic plume.

TABLE OF CONTENTS

1 INTRODUCTION

Volcanic activity constitutes one of the most impressive natural phenomena and has a major impact in their surroundings areas. Volcanoes benefit humanity by fertilizing soils, providing geothermal energy, providing mineral resources and supporting local economies as natural touristic attractions. However, volcanoes also constitute a natural hazard due to increments in their activity. This risk is increased when populated areas are located close enough to an active volcano; tragic events like Mt Peleé eruption (1902) and Nevado Ruiz (1985) evidence their destructive potential.

The volcanic risk can be reduced by a constant monitoring of its activity. For many years several methods have been developed in order to measure geophysical parameters that indicate changes in the volcanic activity, for instance: seismic events, temperature variations, deformation, geochemical composition, gas emissions, etc.

Gas emissions are an interesting parameter due to its strong correlation with changes in volcanic activity and their local effects in human's health, agricultural damage and the production of acid rain. In addition, volcanic gas emissions have a global impact on the atmospheric composition. Currently when the global warming issues have got special attention, it is important to characterize the contribution of the volcanic emissions to this phenomenon in order to have a better estimation of the anthropogenic impact.

Traditionally volcanic activity indicators are measured in situ, meaning a direct contact with the measured parameter. This situation is often a limitation for an adequate research work due to the high risk of being close to an active volcanic vent. The tragically incident of mount Galeras in 1990 where six researchers lost their lives illustrates this reality.

Remote sensing techniques offer an attractive option for volcanic observation without risk of human injury. Satellite remote sensing has been applied to monitor volcanic activity including gas emissions with interesting results However, satellite imagery has a very limited spatial and temporal resolution and their high detection limits only allow us to monitor major eruptive events. For monitoring background gas emissions, ground based remote sensing instruments provide a more accurate alternative compared to satellite measurements.

Sulfur dioxide (SO_2) is one of the main volcanic gases; its presence is an indicator of magmatic activity. During more than two decades SO_2 has been remotely monitored using correlation spectroscopy (COSPEC). Initial measurements consisted of mobile measurements underneath the plume with a fixed telescope pointing to the zenith. This methodology came out with interesting results; but it has the disadvantage of low temporal resolution due to the time required to complete a transverse, especially in areas with limited accessibility and practical limitations considering that COSPEC is a bulky instrument.

Recently this technique has been upgraded and the COSPEC has been replaced with portable spectrometers that are considerably smaller. These instruments detect the gas

columns applying DOAS (Differential Optical Absorption Spectroscopy); a tool that has been successfully applied for the analysis of the chemical composition of the gases in the atmosphere for 3 decades [Platt, Stutz, 2008]. Mini-DOAS is a setup intended to measure gases doing transects under the plume, but in the same way as COSPEC, it has the disadvantage of low time resolution. Following technological improvements this technique has been upgraded; and stationary scanning stations have been developed using the same physical principles of DOAS. This technique named SCAN-DOAS improved the time resolution significantly, since there is a constant monitoring of the volcanic plume and it can work unattended. A significant part of this development was achieved during the execution of the DORSIVA-Project (Development of Optical Remote Sensing Instruments for Volcanological Applications), a European founded project (2002-2005). Based on the success of the DORSIVA project, the NOVAC project (Network for Observation of Volcanic and Atmospheric Changes) has monitored about 20 volcanoes around the world using fixed scanning instruments; thus, providing an exceptional data set based on this novel instrumentation (2006-2010).

However, the deployment of a network of measuring instruments presents a major challenge because of the general requirements of a permanent station. The installation of a local network in a specific volcano demands a very careful planning and time. A typical installation campaign requires either few days or several weeks depending on the geographic-logistic conditions. Moreover; there are volcanoes that increment their eruptive activity unexpectedly; in many cases this situation represents a crisis in terms of human risks. Under such when time is a critical limitation circumstances it is even harder to set up a monitoring network.

Installing a monitoring network demands logistics and transportation; something complicated in areas with very limited accessibility. For instance Sangay Volcano is one of the most active volcanoes in Ecuador, but due to its isolated location in the east flank of the northern volcanic zone of the Andes mountains, permanent monitoring has been difficult to implement.

The difficulties mentioned above about installing time and limited accessibility led to the idea of a rapid deployment network for volcanic gas monitoring using scanning instruments. Other types of rapid deployment networks have been proposed before, but the success of this idea has been depending on the technological limitations at that time.

This thesis demonstrates the use of new technological improvements allowing us to setup a measurement system that can be quickly installed and also provides global accessibility. This document describes the design and implementation of this local network of instruments demonstrating its applicability in a field campaign. We measured SO_2 emissions from Telica, an active volcano located in western Nicaragua, and therefore, providing the first continuous data-set of SO_2 fluxes from this volcano.

Additionally a short term experiment work was conducted at Popocatepetl volcano (Mexico) in connection with a field-campaing in the Fiel volcan project. In this second activity, the rapid installation capabilities of the system allowed us to keep constant tracking of the volcanic plume despite of normal variations of the wind direction.

2.1 The DOAS Principle in atmospheric measurements

Absorption spectroscopy is a technique to measure the absorption of radiation interacting with matter as a function of wavelength. The simplest way to describe the interaction of light with matter is by the classical Beer-Lambert law (equation 1.1).

$$I = I_0 e^{\sigma_\lambda c l} \quad (1.1)$$

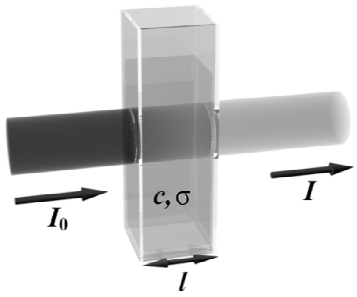

Figure 1. Graphical representation of the beer-lambert law.

Figure 1 shows the physical schematic of the beer-lambert law. I_o is the light source and I is the measured light after it pass through a layer of thickness l . This layer could be any material (gas, liquid) with an absorption cross-section σ_λ and a uniform trace concentration c. The symbol σ_λ denotes the fact that the cross sections are wavelength dependents. The cross-section is a characteristic property of the species under measurement. Two different light measurements, one through a gas layer, another one that is not including a gas layer and knowledge of the cross section of the gas to be studied is enough to know the trace gas concentration (equation 1.2).

$$C = \frac{ln\frac{I_0(\lambda)}{I(\lambda)}}{\sigma l} \quad (1.2)$$

The previous setup can be easily applied in laboratory measurements. However, in the open atmosphere beside absorption, scattering is an important process that interacts with radiation. Scattering is the process by which small particles suspended in a medium of a different index of refraction diffuse a portion of the incident radiation in all directions. In atmospheric measurements the most important scattering processes are Rayleigh and Mie.

Rayleigh scattering mainly consists of scattering from atmospheric gases. This occurs when the particles causing the scattering are smaller in size than the wavelengths of radiation in contact with them. This type of scattering is wavelength dependent. As the wavelength decreases, the amount of scattering increases. This process can be experienced in our daily life by observing the color of the sky. The visible spectrum has shorter wavelengths in the blue region; because of that the sky appears blue since blue

light is scattered more than the rest of the visible light. For the same reason, UV light is scattered about 16 times more compared to the red light.

Mie scattering is caused by pollen, dust, smoke, water droplets, and other particles. It occurs when the particles causing the scattering are larger than the wavelengths of radiation in contact with them. This process can be distinguished by observing the white appearance of the clouds.

Absorption and scattering processes both contribute to extinction of light; therefore equation 1.1 does not represent a realistic model of the interaction of light in the atmosphere because this equation neglects scattering. Although scattering has nothing to do with absorption, because of its contribution to the light extinction it is possible to consider scattering as an absorption process. A more realistic expression can be derived from equation 1.1 including Rayleigh and Mie cross sections: $\varepsilon_R(\lambda)$ and $\varepsilon_M(\lambda)$.

$$I(\lambda) = I_0(\lambda)e^{-l.[\sigma(\lambda).c+\varepsilon_R(\lambda)+\varepsilon_M(\lambda)]}.A(\lambda) \quad (1.3)$$

Equation 1.3 is an extension of the Lambert-beer law including the light extinction caused by scattering. This expression also considers instrumental effects by a proportional factor A(λ), an unavoidable situation in any kind of measurements.

Equation 1.3 assumes that there is just one absorber, but in the atmosphere several other gases can absorb light in similar wavelength regions. Considering all the absorbing gases in the atmosphere that shares the same absorbing wavelength region, equation (1.3) is extended to equation 1.4.

$$I(\lambda) = I_0(\lambda)e^{-l.[\sum \sigma(\lambda).c+\varepsilon_R(\lambda)+\varepsilon_M(\lambda)]}.A(\lambda) \quad (1.4)$$

Equation 1.4 assumes a previous knowledge of the absorbing cross-sections of the different gas species at a particular wavelength region. Gas cross section can be determined in laboratory measurements using high-resolution spectrometers under controlled environmental conditions (Figure 2).

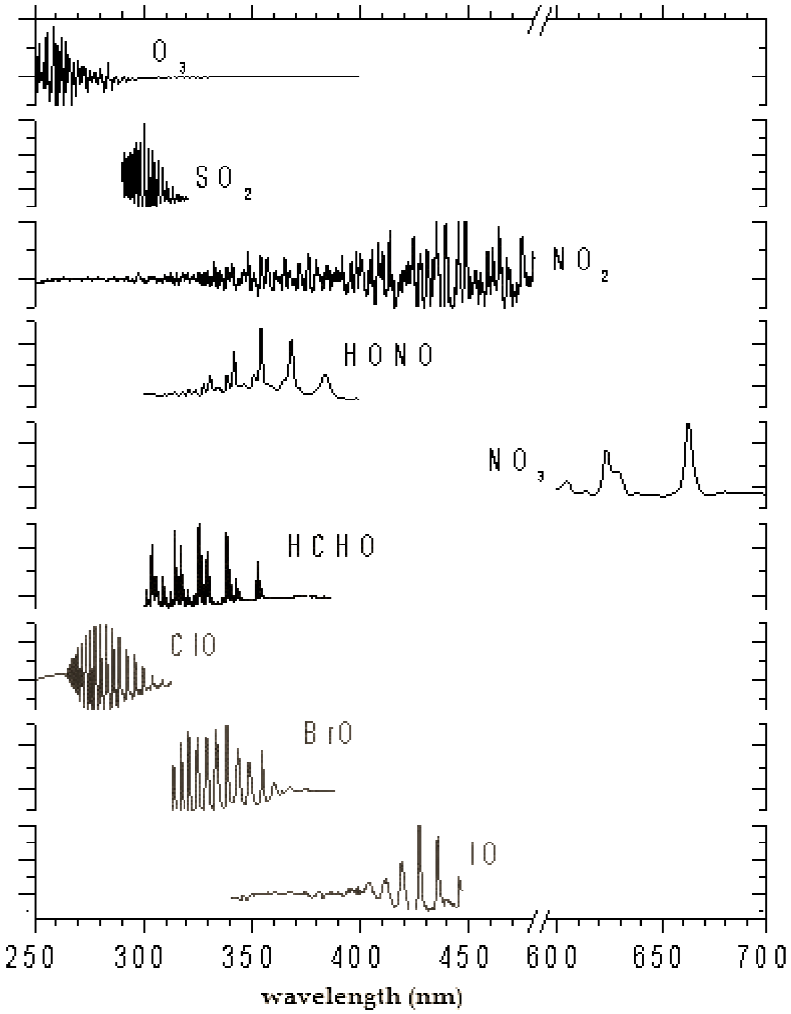

Figure 2. Absorption cross sections of different atmospheric species

An important characteristic of DOAS is based on the fact that several wavelengths (spectral region) are analyzed simultaneously. Doing ground based atmospheric measurements I_o could be difficult to measure; however Figure 2 shows that each gas cross section has a very well defined shape, as a fingerprint. These rapid variations of the absorbing intensity along its wavelength region can be considered as a narrow band structure from a signal processing approach. An atmospheric measurement contains the effect of the absorption and the scattering as a whole; this is illustrated in Figure 3 and equation 1.5. Hence; rapid variations (narrow band) in the measured absorption spectrum is the effect of the gas cross section; on the other hand, slow variations (broad band) in the same spectrum are related to the overall effect of Mie and Rayleigh scattering processes as well as broadband gases absorption.

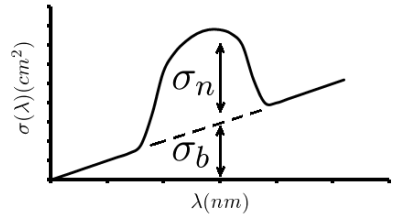

Figure 3. Narrow and broad band of absorption cross section

$$\sigma = \sigma_b + \sigma_n \quad (1.5)$$

Substituting equation 1.5 in equation 1.4 and separating the broad and narrow band logarithmic properties the overall optical density is expressed as an addition of narrow and broad band components as a function of wavelength (equation 1.6).

$$ln\frac{I_0}{I} = l.(\sum_i \sigma_n.C_i) + (\sum_i \sigma_b.C_i) + (\varepsilon_R(\lambda) + \varepsilon_M(\lambda)) - ln(A(\lambda)) \quad (1.6)$$

The foundation of DOAS retrieval consists in separating the narrow band structures by subtracting the broad band structures in the absorption spectrum. The narrow band structures contain the characteristic fingerprint that defines the presence and the amount of a specific gas in the measured wavelength region. The broadband structures can be easily removed applying a high pass filter routine to equation 1.6; afterwards, the optical density D is simplified as in equation 1.7:

$$ln\frac{I_0}{I} = D = l.(\sum_i \sigma_n.C_i) \quad (1.7)$$

Based on the type of light source there are 2 different DOAS techniques: Passive DOAS and active DOAS. Active DOAS uses artificial light while passive DOAS has a natural light source (sunlight, moonlight, stars, etc). Although both methods have their strengths and weakness, active-DOAS implementation could be more challenging due to its technical requirements (synchronizing a light source and an optical receiver). On the other hand, active-DOAS does not depend on the availability of the light source; therefore in principle is possible to measure continuously 24 hours a day. Passive-DOAS is simpler to implement than active DOAS because only a receiver element is necessary. However; passive DOAS is very sensitive to environmental conditions that can affect the instrument performance and in many cases the measurements period are very short since passive-DOAS depends of the availability of the light source. For example in the case of measurements that use the sunlight as a light source, it is not possible to measure during the night.

2.2 Instrumental Calibration

The most important instrument in DOAS is the spectrometer that measures the light intensity at different wavelengths. Typically the modern spectrometers display the spectrum as an array of channels, each of them representing a specific wavelength and its corresponding intensity. However; as any other measuring instrument, the spectrometer must be calibrated; it means relating each channel number with its corresponding wavelength. This can be done using mercury lamps, which have very well known spectral lines; therefore, they are frequently used as a calibration reference for spectrometers in the 300-400 nm UV-range.

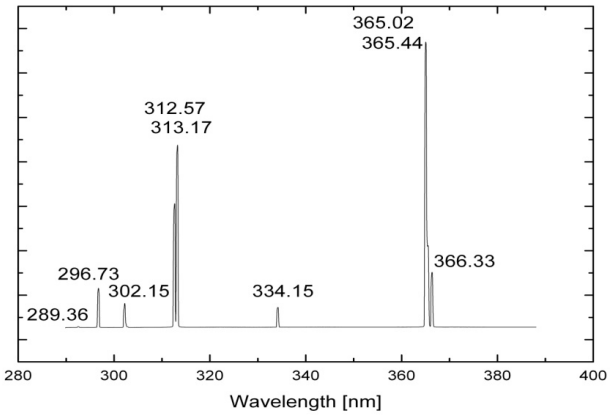

Figure 4. Emission lines of a mercury lamp in the UV-region

The channel number and its corresponding wavelength are related by a fitting polynomial function

$$y = a_0 + a_1 x + a_2 x^2 + a_3 x^3 \quad (1.8)$$

Where:

y=wavelength (nm)

x=channel number

Figure 4 shows a mercury spectrum from a real spectrometer, in theory the width of the emission line should tend to 0 as a delta-Dirac function. In practice; the measured spectral line rather has a Gaussian shape due to the physical limitations of the wavelength resolution of the instrument, this physical property inherent to all the spectrometers is called the slit function.

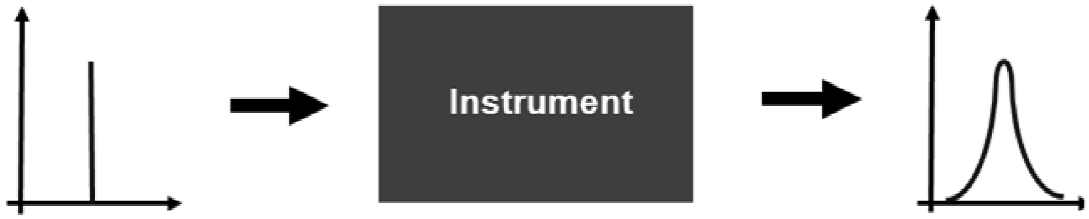

Figure 5. Physical response of the instrument to a spectral line

The Convolution is a mathematical expression that allows characterizing the instrument response from any signal by relating the measured spectrum and the slit function.

$$Y(\lambda) = h(\lambda) * I(\lambda) \quad (1.9)$$

Where:

Y=physical output

h=Slit function

I= Spectral line

Convolving the high-resolution cross section of a specific gas (Figure 2) with the slit function of a particular spectrometer produces a reference file of the trace gas adjusted to the physical properties of that spectrometer.

2.3 DOAS retrieval

DOAS retrieves the gas column densities by distinguishing between broad-band and narrow band structures of the considered spectral region (equation.1.6). The narrow band structures are separated by applying a high pass filter algorithm to the optical density; thus, removing the broad band structures of the spectrum. Afterwards the reference cross-section is fitted to the optical density applying a curve fitting algorithm (Figure 6). The outcome of the fitting routine is an amplitude coefficient (Column Density) that corresponds to a value that minimizes the difference between the convolved cross-section and the measured optical density. The goodness of the fitting is evaluated using the chi-square test (equation 1.10).

$$\chi^2 = \frac{\sum_i^K (C.\sigma(\lambda_i) - D(\lambda_i))^2}{D(\lambda_i)} \quad (1.10)$$

In practice, several software tools retrieve measured spectra applying these procedures: WinDOAS [Roozendael; Fayt, 2001], and DOASIS [Kraus, 2005] among others.

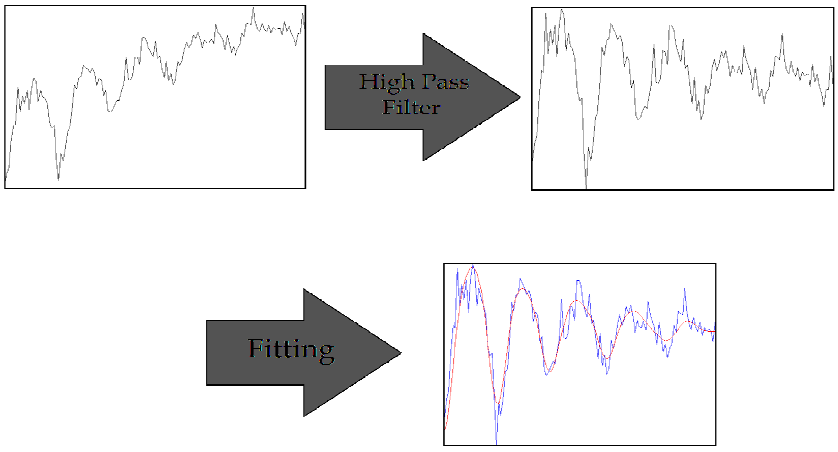

Figure 6. Example of SO_2 Column Density retrieval: high pass filtering of the optical density and curve fitting of the SO_2 cross section

2.4 Volcanic Flux measurements

In the previous section a basic approach to the concepts of DOAS was exposed considering that this is the measurement technique applied in this work. On the other hand, some previous work have demonstrated the relevance of SO_2 as an important indicator of volcanic activity [Symonds et al., 2001; Olmos et al.,2007], therefore volcanic SO_2 flux measurements is the main focus in this work. Laboratory measurements of the SO_2 absorption cross-section have reported that this trace gas has a very well defined absorption structure in the UV region (≈300-320 nm) [Stanley et al.,1993; Vandaele et al.,1994].

Measuring in the UV-region has also the advantage of using the scattered atmospheric light as the light source. This arrangement is possible for measurements in lower altitudes whereas it is possible to estimate the absorption spectrum across a relative small gas plume emitted from a point source like a volcano, or a chimney in a factory (Figure 8). In this case, the reference spectra or clean air; can be taken by pointing the instrument away from the gas plume

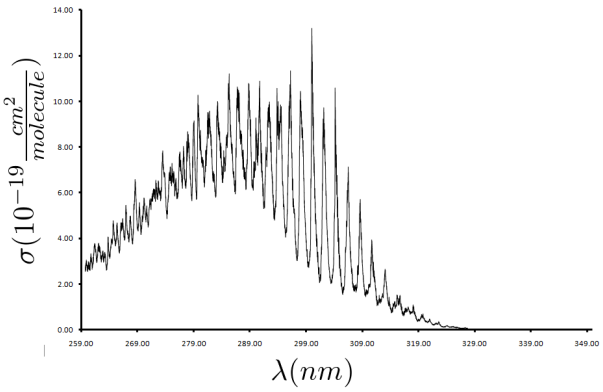

Figure 7. SO_2 Cross-section in the UV region [Vandaele; 1994]

The direct outcome from DOAS measurements are the column densities (V) that can be defined as the concentration (C (z)) of a trace gas along an interval of the atmosphere.

$$V = \int_{z_1}^{z_2} c(z)dz \qquad (1.11)$$

The interval Z_1 –Z_2 can represent an atmospheric layer (for instance the stratosphere or troposphere), or a smaller interval like a volcanic plume.

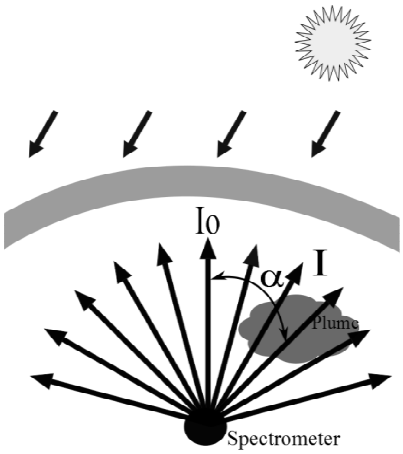

Figure 8. Schema of a gas column measurement. An spectrum with clean air (I_o) is measured. Afterwards sequential measurements of UV across the volcanic plume (I) are taken and compared with the clean air spectrum.

The column densities do not provide enough information to estimate the gas flux; in addition, is required: wind speed, wind direction and in many cases plume height depending on the measurement strategy. Wind data can be obtained by direct measurements or using meteorological archived information, while plume height is possible to retrieve from a geometrical approach. Mobile-DOAS and scan-DOAS measurements both are measurements strategies used for volcanic and anthropogenic gas emission measurements at lower altitudes.

2.4.1 Mobile DOAS measurements

This measurement strategy is based on measurements from a mobile instrument; a typical setup consists in a spectrometer with a telescope pointing to the zenith and collecting spectrum while it moves below the plume. The spectrum is collected in a Laptop and the distances and direction travelled are estimated by using a GPS.

The flux is calculated assuming a homogenous distribution of the molecules along the light path and applying the DOAS equation for retrieving column densities (equation 1.11). For this measurement strategy, where the spectrum is acquired pointing to the zenith, the column densities are termed as Vertical Column Densities (VCD), and converted from ppmm into mass units (mg/m^2).

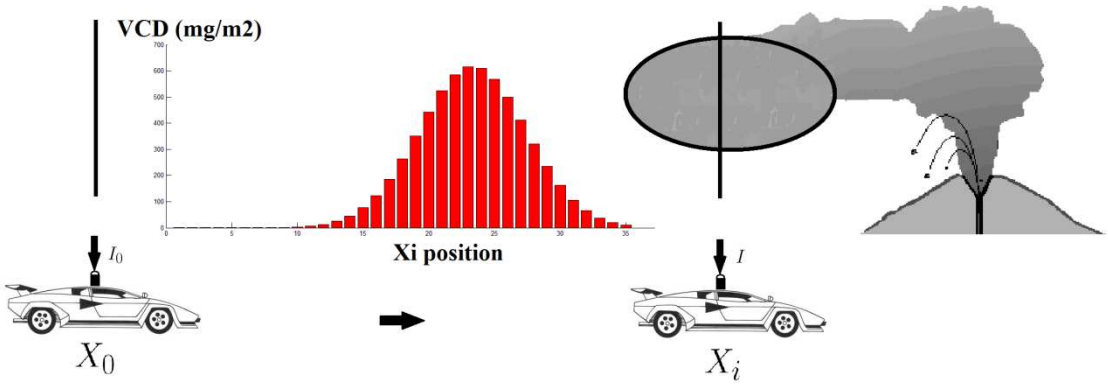

Figure 9. Schema of Mobile-DOAS flux measurements

$$Flux = \int_{X_i}^{X_n} VCD(x).W_s dx \quad (1.12)$$

Where:

X_i –X_n: is the travelled distance behind the plume

VCD(x): are the individuals vertical column densities at a position x

W_s : Wind Speed at plume height

In practical terms equation 1.12 is redefined for n individual vertical column densities:

$$Flux = (\sum_{i_0}^{n} VCD_i.\Delta x_i).Ws \quad (1.13)$$

Finally the resultant flux is corrected in terms of the Wind Direction (W_d) and moving direction(M_d) :

Corrected Flux=Flux(COS(W_d-M_d))

Depending on the conditions the traverses can be done either using a car or just walking. The main advantage of this measurement strategy is that not fixed installation is required and it can be easily implemented in case of eventualities. However; this setup has the disadvantage that it cannot be implemented automatically, the time resolution is poor and in some cases, there are not adequate roads around the emission source.

2.4.2 Scan-DOAS measurements

This technique consists of several measurements from a fixed point across a gas plume. In contrast with the mobile DOAS where all the gas columns are measured vertically, the scan DOAS measures column densities (equation 1.11) at different angles. In this the column densities are called Slant Column Densities (SCD). Adding up the measured SCD at different angles, we can retrieve the concentration of the gas plume (Figure 10).

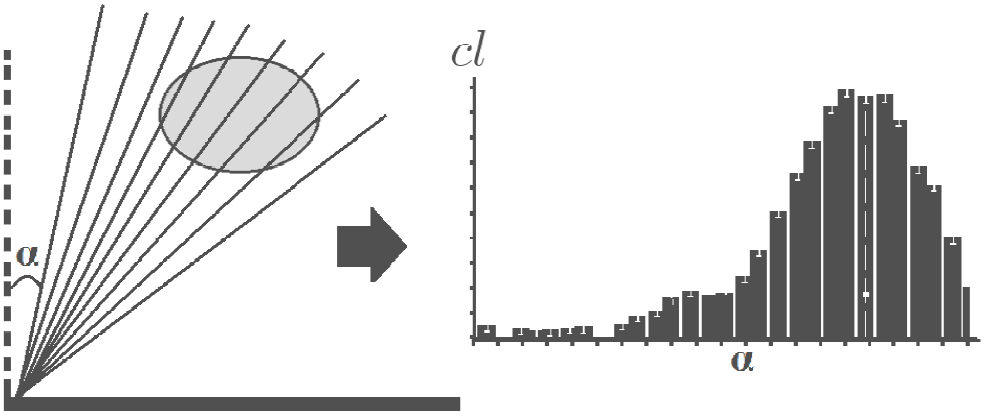

Figure 10. Measurements of slant columns at different angles; sketch the cross section of the volcanic plume

As in mobile DOAS, the slant columns alone do not provide enough information in order to estimate the gas flux; meteorological data is also required: wind speed and wind direction. In addition the plume height is also necessary. Wind data can also be obtained from meteorological archived information. However, an advantage of the scan DOAS is that is possible to estimate geometrically the plume height and wind/plume direction when two separated instruments are running simultaneously. This estimation can be done by observing in each instrument, the angle of the slant columns measurements that corresponds to the plume center. A previous knowledge of the instrument and crater locations is required in order to perform this geometrical approach (Figure 11).

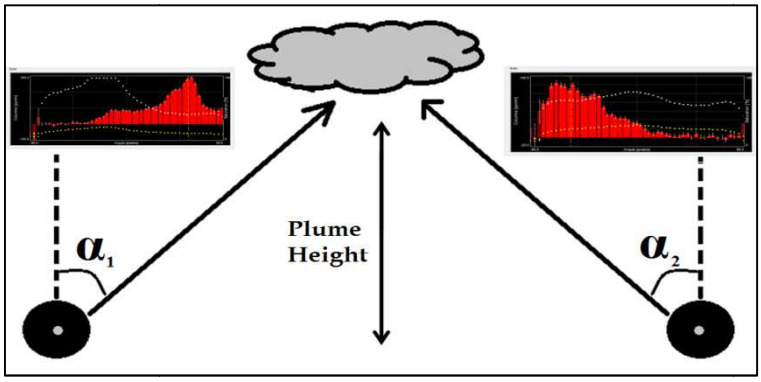

Figure 11. Geometrical location of the plume height from the angular direction to the center of the plume

For flux retrieval is is necessary to convert the slant columns densities to vertical column densities (VCD). This is done for every two adjacent SCDs, multiplying each column by the cosine of its scanning angle α_i and averaging all the pairs of measurements (equation 1.14) .

$$\overline{VCD}_i = \frac{S_i cos\alpha_i + S_{i+1} cos\alpha_{i+1}}{2} \quad (1.14)$$

In the simplest case, the flux is calculated according to equation 1.9:

$$Flux[\frac{mg}{s}] = h_p * ws\,|\cos(wd - compass)| * (\sum_{i=0}^{N-1} |\tan(\alpha_{i+1}) - \tan(\alpha_i)| * \overline{VCD_i}) \quad (1.15)$$

Where α_i correspond to the angle of the Slant Column Density relative to zenith, N is the amount of measurements per scan, wd is the angle of the incoming wind direction, compass is the direction from the scan towards the volcano and the and ws is the wind speed at the plume height(h_p) [Johansson et all, 2009].

2.4.3 Installation of Scan-DOAS systems.

The main advantage of the Scan-DOAS as a measurement strategy is that it can be acquiring spectrum continuously; therefore, improving the time resolution. However, a disadvantage is that normally a fixed scaning-DOAS installation takes some time before being completed. It is important to have a previous knowledge of the yearly average of the wind direction at the volcano; therefore, the installation area should be located downwind in order to capture the plume. Also the places where the instruments are assembled must have a clear horizon free of obstacles like trees and buildings and naturally, in a secure place. Finally the instrument view direction (azimuth) must be oriented pointing towards the crater, since this is the emission's source. The process of identifying the places that fulfill the installing conditions mentioned above in addition to the construction of a proper infrastructure can be completed from a few days to a few weeks. The main purpose of this thesis work is focused on the implementation of a network of scan DOAS instruments that reduce all the possible delays described above in case of a volcanic crisis

3 System Design

The theory explained on the previous sections had the purpose to provide a basic background of the physics related to the design and implementation of a real instrument. However, most of practical implementations involve technical challenges and design considerations. This chapter deals with the most relevant aspects that were considered during the design stage of the rapid deployment system.

3.1 General description.

In simple words, the system consists in a local network of ground based instruments and a central processing-communications unit. Figure 12 shows the system's topology.

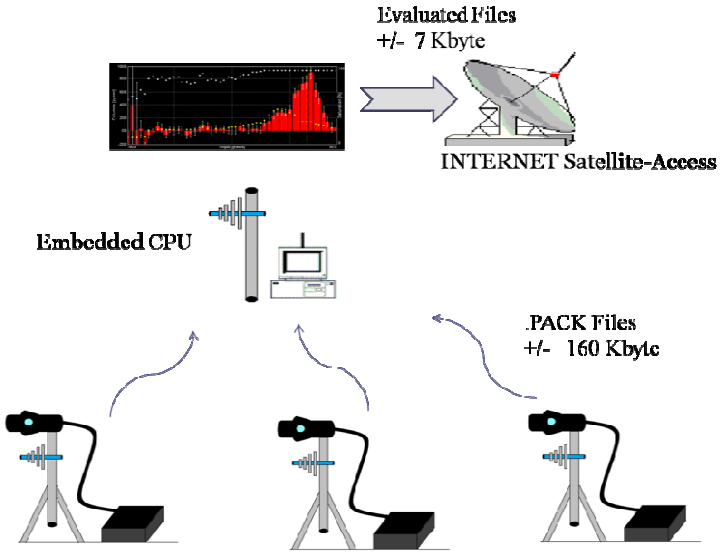

Figure 12. Rapid Deployment System: general framework.

The main characteristics of this set-up are:

- Flexibility: The installation can be modified easily according to the measurements requirements.

- Portability: The system should be installed/uninstalled in case of any volcanic crisis

- Embedded processing: The main computer generally is located in an observatory, away from the instruments; we replaced this by a portable computer that process the data in situ and work unattended.

- Accessibility: The data must be accessed from any place.

Two main units were built to fulfill the characteristics described above.

- Instrument unit: Scanner, spectrometer and electronic box.

- Process and communication unit: Embedded computer, and satellite link

The process unit accesses the instruments by a radio link; the information is recorded and processed in the embedded computer. The purpose of processing information in situ is to produce a smaller amount of data compared to the raw data; thus, reduce the cost of satellite transfer of data. A raw file containing the spectra and time information weights about 160 Kbytes. After the evaluation process, the information is resumed in a file that weights about 6 Kbytes, meaning a compression of about 96%. This reduction in the cost of transferring data is achieved because the satellite transmission costs is based on the amount of transmitted bytes; therefore, sending evaluated data by a satellite link is less expensive and faster than sending raw data.

3.2 Instrument unit.

This unit is main core of the system, it acquires and store spectra at different angular positions implementing the measurement strategy discussed in the previous section: optics, spectrum acquisition, mechanical control of the scanning system, and UTC synchronization.

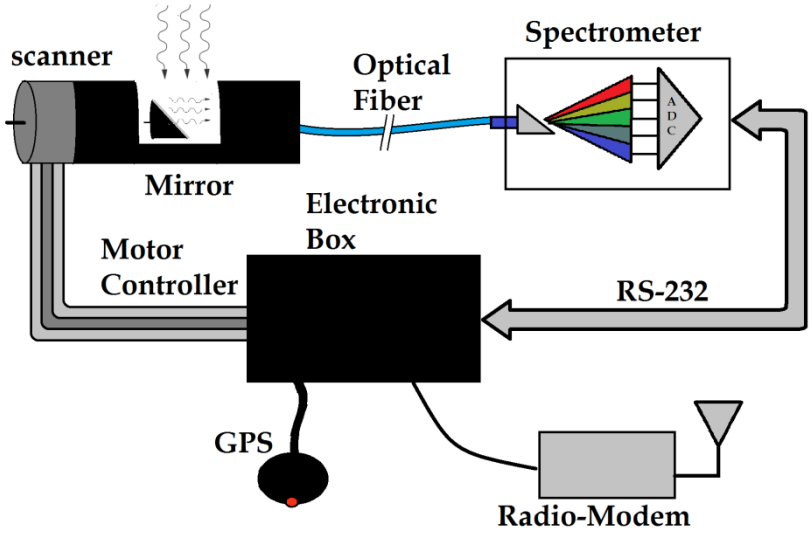

Figure 13. Schematics of the instrument Module

3.2.1 Scanner

This is an opto mechanical device that measures the slant columns at different angles and transmits the light to the spectrometer. It consists in mirror or a prism coupled to a stepper motor that rotates 3.6 degree/step; the light is redirected either by a mirror or a prism to a telescope. The telescope consists of a 75 mm focal length quarts lenses that couples the transmitted light to either one or two optical fibers with 600 μm diameter

located in the focal plane; hence, a field of view of 8 mradiis is achieved. In addition, visible light is filtered out using a UV band pass filter mounted in the telescope. Finally the light is transmitted to a spectrometer by the optical fiber.

The mirror can scan a plume perpendicularly to the optical axis of the telescope or with a different inclination, typically 60 degrees. These two modes of operation are termed flat-or conical scanning.

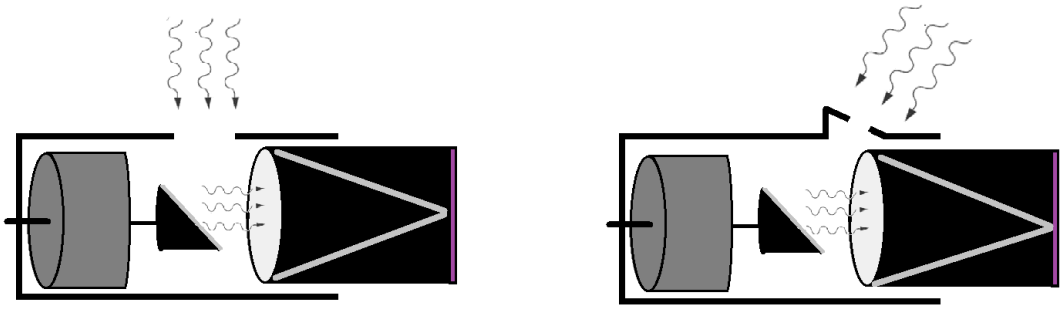

Figure 14. Schematic of the scanner (Flat and Conical), notice the the inclination of the incoming light.

Any of these angular configurations can be used for the same purpose; however when an instrument is installed it is possible to take advantage of their angular characteristics in order to avoid obstacles at the horizon like tress or buildings that can cause blocking of the field of view. In addition, some experiments have reported that conical scanners are more sensitive compared to the flat scanners to detect the volcanic plume when the plume direction turns slightly away from the azimuth direction of the scanner. This is because the distance from the instrument to the plume is shorter compared to the flat configuration due to its angular inclination; therefore, reducing the effect of plume dilution [Johansson et al, 2006]. On the other hand, the flat scanner is more accurate for the geometrical estimation of the plume height; in addition, a special set up of a flat scanner with two optical fibers and a double channel spectrometer can perform wind speed measurements when the plume direction is stable above the instrument. This arrangement captures two different spectra that are time delayed. Correlating the time delay it is possible to infer the plume speed as long as the plume is located above the scanner (Figure 15).

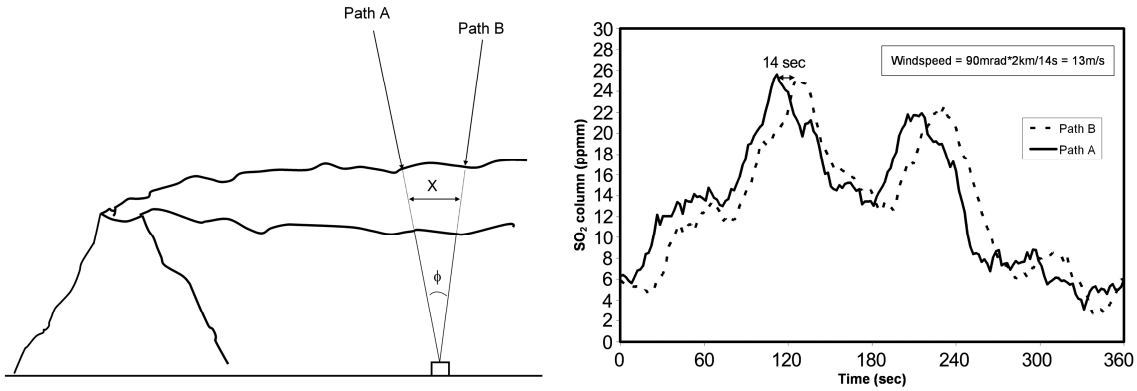

Figure 15. Wind speed measurements using a double beam flat scanner. The wind speed can be inferred by calculating the time delay of the column measurement between the two beams (Galle et al, 2006).

3.2.2 Spectrometer

The spectrometer receives the incoming light from the scanner via the optical fibers and converts the spectrum to a digital signal for further processing and storage. Considering that the absorption of SO_2 has its stronger "fingerprint" in the UV region (300-320 nm), the spectrometers Ocean Optics S2000 or SD2000 are grating spectrometers suitable for UV spectroscopy. The entrance slot of 50 μm yields a resolution of about 0.6 nm in the range of 280-410 nm. The detector is a Sony ILX511 CCD-linear array of 2048 pixels that allows adding up to 16 cconsecutive spectrum measurements for noise reduction. The CCD array is sequentially transferred to an analogue-digital converter (ADC) with a resolution of 12 bits. The integration time can be controlled by external software commands in order to obtain a better performance in terms of light intensity and saturation.

Optical Signal to Noise relation	250:1
Power Consumption	5V, 650 mW
Integration Time	2-30000 mS
ADC resolution	12 bits
I/O	USB,RS232
FWHN (Resolution)	0.6-0.8 nm
Range	280-410 nm
Grating	17
Focal length	42 mm (input) 68 mm output
Well depth	160,000 photons

Table 2.1 Technical characteristics of the spectrometer S2000

3.2.3 Electronic box

This device performs a sequential control of the spectrum measurements, data storage, GPS, scanner motion, voltage and temperature measurements.

The kernel of this device is an embedded computer AXIS 89 with Linux 2.6 as operative system, 200 MHz RISC AXIS CPU processor, HTTP and FTP servers, 32 Mb RAM, 4 GB memory in an external CF card, a digital I/O interface, 2 ethernet ports and 3 RS232 ports. In addition the box has an external power interface to drive the stepper motor, the voltage/temperature sensors, the GPS and the spectrometer.

A typical measurement sequence is as follows:

- The stepper motor rotates and directs the field of view of the scanner to the zenith and the exposure time of the spectrometer is automatically set to typically 80% of saturation. Normally in sunny conditions the exposure time is about 150-450 milliseconds.

- A Sky spectrum is recorded adding up normally 15 spectrums.
- The scanner rotates 180 degrees (nadir) in order to record a dark spectrum.
- A scan is formed when spectra are recorded every 2 motor steps (3.6˚) completing and arc of 180˚. In total there are 52 spectrums recorded including the zenith and the dark.
- All the spectra, GPS record, voltage and temperature date are stored in a compressed *.pak file.
- A new cycle is repeated

The pak file size is typically about 140 Kbytes; therefore, it is possible to store in the flash memory data from two months of measurements. The file contents raw data without any level of processing. Data evaluation requires higher computing resources; therefore, this task is assigned to a central computer with more processing capabilities.

3.2.4 Local Wireless Communication

The raw data must be transferred from the instrument to a central computer in order to be processed. In most of the NOVAC installations, the central computer is located at a volcano observatory dozens of kilometers away from the volcano. One of the most important features of the rapid alert system is that the central computer is portable; therefore, it can be located relatively close to the installation area. This reduces the complexity of installing a local wireless network. In normal cases, setting up a communication network could be a challenge mostly in areas where the terrain is surrounded by obstacles, and even more during a volcanic crisis.

The electronic box can be either accessed by Ethernet or RS232. Ethernet has a faster baud rate and a radio link can be implemented using a WLAN. However, WLAN typically operates at 2.4 Ghz (IEEE 802.11) meaning a higher power consumption and also requires better topographic conditions between two points. At higher frequencies the open path gives higher loses; requiring high gain antennas. The antenna gain is proportional to its size; thus, such antenna in most cases is not a portable device, rather requires some kind of infrastructure. On the other hand a radio link that operates at low frequencies is less affected by minor obstacles likes vegetation and bad weather conditions.

For data transfer, RS232 is a flexible communication protocol that can be very easy adapted to a wireless network. The most practical way to implement a wireless network for RS232 protocol access is using serial Radio-Modems, this is a feasible way when a quick installation is required; furthermore, the electronic box described in the previous section has its own file transfer protocol over RS232.

In our particular case, the local network was made using Frewave FGR115-RC radio modems. These radios have two models available; 900 Mhz or 2.4 Ghz band and are based on Spread-Spectrum techniques meaning a more robust and secure radio network. Although the 900 Mhz band is a better option than 2.4 Ghz because of the advantages of

operating at lower frequencies, local radio frequency regulations in some countries force the use of 2.4 Ghz radios.

The Ethernet ports of the electronic box can be optionally used for fast manual downloading of data in case of a failure in the wireless communication network.

3.3 Data Processing Unit

This module has the task to process the raw data coming from the instruments and transmit evaluated files by a satellite link; thus reducing the cost for the satellite data transfer. Processing data in situ requires a portable computer with enough resources to run DOAS evaluation routines and the capability to work under hard environmental conditions.

3.3.1 Embedded Computer

The implementation of the least square-routines for the flux evaluation demands considerable computing resources. Traditionally, this task has been done by a desktop computer or a Laptop executing the NOVAC Program [Johansson; Zhang, 2005]. For an application that requires that data is evaluated in situ, neither desktop computer nor laptop is a suitable solution. Both possibilities are high power consumers, and even a laptop is not good enough. Moreover, they are not designed for outdoors operations beside the fact that are attractive objects for stealing.

A few years ago there were no possibilities to evaluate spectrum in situ unattended, but recent technological developments have created embedded computers with enough computing resources capable to run windows based applications. The embedded computer PCMB-6684 from NORCO Company fulfills our requirements of portability, enough computational resources and low power consumption based on its technical specifications (table 2.3).

Processor	Onboard: AMD LX 800 Frequency: 500 MHz
System Memory	Onboard 4x 64MB DDR 333MHz
Board Size	96mm×90mm
Power Requirement	5V /12V ; 6W
Operating Temperature	(0℃~60℃)
Storage	Type CompactFlash, Support DMA , 4GB
I/0	4xUSB, 2xRS232, Ethernet
Heat Dissipation	Fanless
Operative System	Windows 2000

Table 2.3 Technical Specifications of NORCO embedded computer

Power consumption is a compromise between computing power and application requirements; considering that the NOVAC software does not need more that what this computer provides, this board is suitable for our purpose. Low power consumption (6 W) is possible because data storage is not based on a mechanical hard-drive disk, but on a flash memory hard-drive which also has the advantage that there are no moving parts inside that produce heat and vibrations. Solid state storage devices are more robust to electromagnetic interference and are also more suitable to endure hard environmental conditions like temperature, altitude changes and dust. In addition the heat dissipation mechanism of this processor is fanless; avoiding using fan coolers; therefore, the power budget is even more reduced

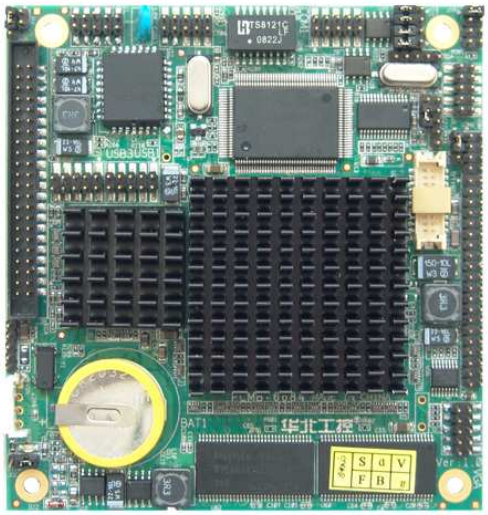

Figure 16. Embedded Motherboard

3.3.2 Automatic control

Since this is an application of passive-DOAS, the measurements are made only during daylight. This is controlled by an electromechanical timer that activates the instrument every morning, and also stops it after the sunset. Because the system is not running all the time, there is no reason to keep the embedded processor running continuously; and thus wasting energy. For this reason the embedded processing also requires to be turned on/off by an second electromechanical timer. Nevertheless, this is a computer running Windows 2000; and as any operative system, there is a risk of malfunctioning if the computer is turned off abruptly; therefore, it is not recomendable to turn it on/off just by an electromechanical timer. Thus, software shutdown is scheduled in the task manager just before the electromechanical timer turns off the computer.

3.3.3 Data Evaluation and communication.

Each time the computer is turned on, the NOVAC Program automatically starts up and execute the following routines:

1- Download the raw data from the electronic boxes in the embedded unit.
2- Evaluate the data, applying DOAS algorithms
3- Send evaluated data to the NOVAC server

Typically an evaluated file is just 7 KB, in contrast; the raw files from the instrument are 140 KB. Evaluating in situ reduces 96% the file size that is sent to observatories for a posteriori flux calculation.

Wireless communication is the most practical way to provide connectivity to remote areas. But customized radio links are conditioned to terrain features; therefore a particular wireless network requires a very careful planning and also takes some time before it is ready. Cellular networks are present almost worldwide, but even in the most developed countries there are wide remote areas that are not covered. Satellite links provide a global solution for connectivity. Its principal advantage relies on its coverage area. Another advantage is that during a crisis, it has been observed that most of the other commercially available communication services tend to crash as a result of high data traffic [Tárraga et al, 2001]. Satellite links as a resource for crisis management has been proven before in real scenarios [Bowman et all, 2008]. Satellite antennas tend to be bulky and heavy, and not easy to install. New technological improvements have produced portable satellite modules with global covering and internet accessibility. The module that we used is SABRE I, with a baud rate of 384 kbps, Ethernet port and a reduced dimension of 259 x 195 x 58 mm. The global satellite network service is provided by BGAN (Broad Global Accessibility Network) [www.inmarsat.com]. After the satellite link is established the module implements an embedded DHCP server; allowing internet connectivity. The network security settings are configured in a firewall running in the embedded computer.

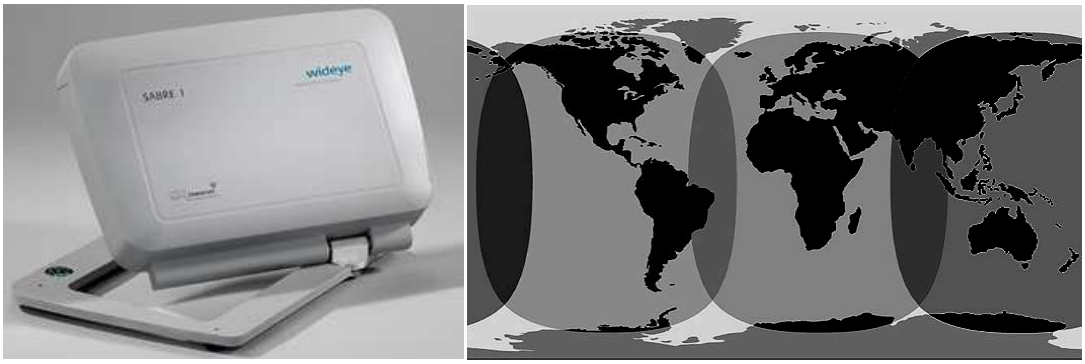

Figure 17. Satellite Module and BGAN coverage.

3.3.4 Power management

In systems that are intended to work in the field, energy access is often very limited; therefore, solar energy is the best alternative in such systems. There are many

commercial products available to fulfill this requirement; but in most cases, solar energy demands some type of infrastructure because solar panels can be heavy and difficult to carry. A portable device also requires portable power supply. Our system uses a foldable-low weight solar energy panel provided by GlobalSolar [http://www.globalsolar.com]. This device is able to deliver up to 60 watts, matching the minimum power demand of the whole system. Electronics components, especially the embedded computer and the satellite module are very sensitive to voltage fluctuations. Hence the power supply of the system has to consider two more requirements: efficiency and electrical stability. The most common used device for this purpose is a traditional power regulator that reduces the output voltage to a constant level. Under nominal conditions these regulators exhibit acceptable voltage stability; but voltage regulation is done by heating dissipation; meaning a very low efficiency. A better solution is a switching DC/DC converter. This device relies in non dissipative components (inductors and capacitors) that temporally stores energy from higher voltages and release it at lower voltage levels. This energy conversion method is more efficient and stable than heating dissipation. The embedded motherboard was powered using a switching DC/DC converter picoPSU-120, capable of driving 80 watts, 96% efficiency and voltage outputs of 5/12 VDC.

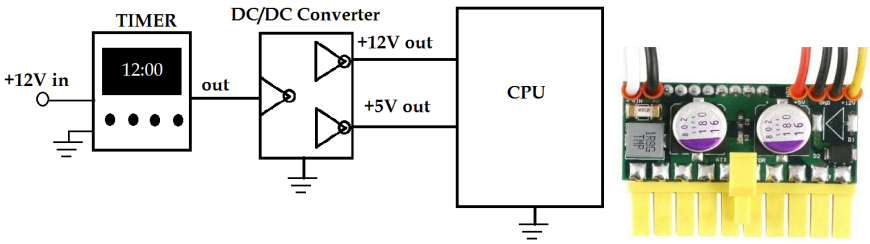

Figure 18. Timer and power system converter picoPSU-120

Figure 19. Foldable 60 watts solar panel

4 Field Applications

4.1 Télica Volcano Nicaragua

Télica is an active volcano classified as a stratovolcano and located on the west of Nicaragua (12.602 N; 86.845W) near to the city of Leon. The crater has an altitude of 1061 m.a.s.l and 700 meters in diameter. This volcano has erupted several times during historical times, with a last eruptive event in 2008. The presence of a visible plume evidenced passive degassing activity at the time of our experiment.

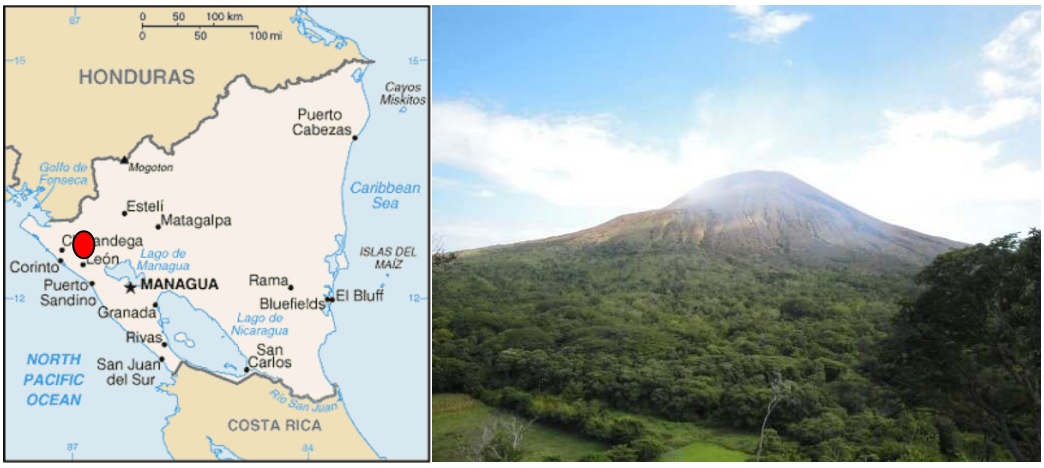

Figure 20. Télica Volcano

As in other areas of Central America, the weather in Nicaragua is characterized by two seasons: a dry season (November-April) and a rainy season (May-October). Good weather conditions are critical for accurate passive-DOAS measurements; thus, the dry season was selected to perform our measurements. During December 2009-March 2010 an intense measurement campaign took place at this volcano. The purpose of this field work was to test the rapid deployment system and get a continuous dataset of gas measurements. Telica volcanic activity is constantly monitored by Instituto Nicaraguense de Estudios Territoriales (INETER) using seismic stations, temperature sensors, and cameras; however, there are no reports of continuous gas measurements; [INETER 2010], only sporadic traverses using COSPEC and Mobile-DOAS.

4.1.1 Identification of installation sites.

The side of the volcano where the instruments were installed was mostly determined by the predominant wind direction. This area in Nicaragua is characterized by an incoming wind from the North-East direction [INETER]; therefore, the installation area corresponds to the south-west side of the volcano. Since the instruments should be working unattended, it was necessary to consider security requirements. A small village named Cristo-Rey is located in the installation area; hence, the instruments were installed in private properties where it was able to get permissions and also free of visible obstacles between the scanner and the volcanic plume.

Figure 21. Installation area around Telica Volcano showing the three sites: Cristo Rey, Mendoza and Los Angeles

4.1.2 Field Installation

Three sites with similar characteristics were finally selected: Cristo Rey, Mendoza and Los Angeles. The 3 instruments where located about 3 km apart at a distance of about 6 km from the volcano. The instruments in the flanks used a conical scanner while the instrument in the center has a flat scanner. This arrangement was made in order to maximize the coverage at different wind directions and ensure a good overlay between the instruments to facilitate plume height and plume direction measurements.

Site	Distance to the Crater (Km): 6.1
Cristo Rey	Altitude (MSL): 256.5
	Latitude: 12.608
	Longitude: -89.898
	Scanner Type: Conical
	Compass direction(º): 100

Figure 22. Installation at Cristo Rey site

Site	Distance to the Crater (Km): 6.5
Mendoza	Altitude (MSL): 232.0
	Latitude: 12.598
	Longitude: -89.902
	Scanner Type: Flat
	Compass direction(º): 75

Figure 23. Installation at Mendoza site

Site	Distance to the Crater (Km): 6.6
Los Angeles	Altitude (MSL): 215.0
	Latitude: 12.578
	Longitude: -86.898
	Scanner Type: Conical
	Compass direction(º): 70

Figure 24. Installation at Los Angeles site

4.1.3 Real time evaluation

The processing unit was placed close to the site Cristo-Rey. From that site, the distance between two points was relatively short (up to 3 km) and the terrain was fairly flat; therefore, high RF power was not required. However, there were small obstacles as trees, fences and houses; in addition the differential altitude between the instruments was not high enough (≈ 20 mts). Under this conditions and because the Freewave modems used in this network, comunicate under a frequency of 2.4 GHz, only the closest instrument to the embedded computer was accessed by a radio link. The data from the other two instruments was manually downloaded.

The average environmental temperature during that season was about 40 ˚C; in addition the equipment was exposed to direct sunlight. The scanning instrument operated properly under these conditions but the module with the embedded computer has a lower temperature threshold, especially at noon, when sunlight reaches its maximum intensity. In order to avoid a malfunctioning of the device, the embedded computer was scheduled to work at two different periods of the day: from 7 to 10 and from 16-18. These periods correspond to the sunrise and the sunset at the local time, when the environmental temperature is generally lower than the daily temperature average. This approach ensured an uninterrupted daily processing and data transmission under

extreme temperature conditions. After a complete day of measurements an average of 160K bytes was sent via the satellite link to the main server in Chalmers.

Figure 25. Data processing unit installed at Cristo Rey

4.2 Popocatepetl Volcano

Figure 26. Popocatepetl Volcano and its location in Mexico

Popocatépetl is an active stratovolcano located in the central area of Mexico. Several historical records even from pre-Hispanic times reveal a latent activity and occasional violent eruptions. Due to its proximity to high populated areas (Puebla and Mexico D.F.) explosive eruptions of this volcano constitutes a natural hazard to about 30 million inhabitants. Popocatépetl volcano is intensively monitored by CENAPRED due to its strong activity. Its monitoring network consists in more than 50 signals including: seismicity, gases and geodesy. [CENAPRED]. During April 2010 a measurement campaign was carried out around Popocatepetl volcano using among other instruments, the rapid deployment system. The purpose of the rapid deployment system in this scenario was to take advantage of its fast installing characteristics in order to keep tracking of the variations of the volcanic plume according to the wind speed/direction changes and measure the SO_2 fluxes.

4.2.1 Field Work

The field work was carried out in the south-east area of the volcano according to the predominant wind direction observed during the time of our experiment [CENAPRED]. The field exercise consisted of daily measurements locating the center of the volcanic plume and setting up temporary installations of scanning instruments at both sides of the plume. This allows the estimation of the plume height and direction according to the geometric approach described in Figure 11 . The scanning measurements were complemented with simultaneous mobile measurements using COSPEC and mobile DOAS. Mobile measurements located the position of the center of the plume, suggesting the possible installation sites for the scanning instruments. Mobile traverses also performed wind speed and plume altitude measurements using the double beam mini-DOAS technique [Johansson et all, 2009]. However reliable double beam wind speed measurements are limited to very stable plume directions.

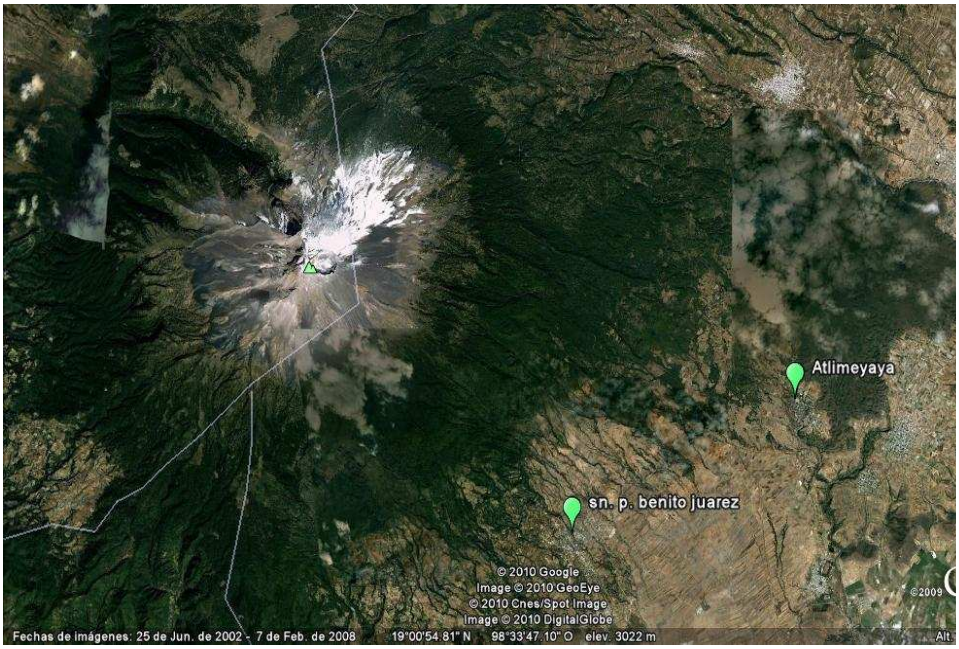

Figure 27. Measurement area in the south-east side of Popocatepetl Volcano

5 Measurement results

5.1 Télica Volcano

As mentioned in section 1.2.2, flux retrieval requires four parameters: the sum of VCD's, wind direction, plume height and wind speed (equation 1.15). Wind direction and plume height can be estimated from the geometrical information from two or more instruments measuring simultaneously (Figure 11). Figure 24 and 25 show the behavior of the wind direction and plume altitude during our measurement campaign.

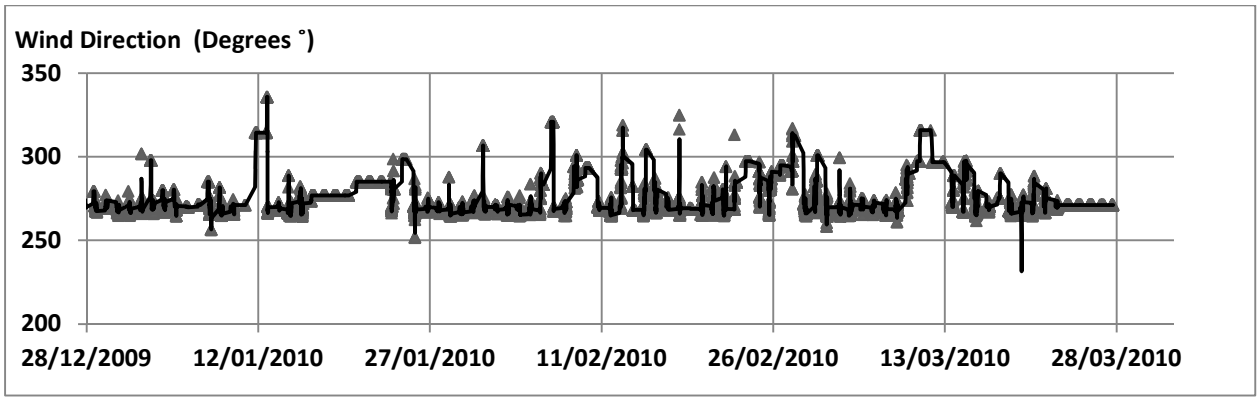

Figure 28. Wind direction (Degrees ˚) during the measurement period. A predominant direction of 270 degrees is observed during this period.

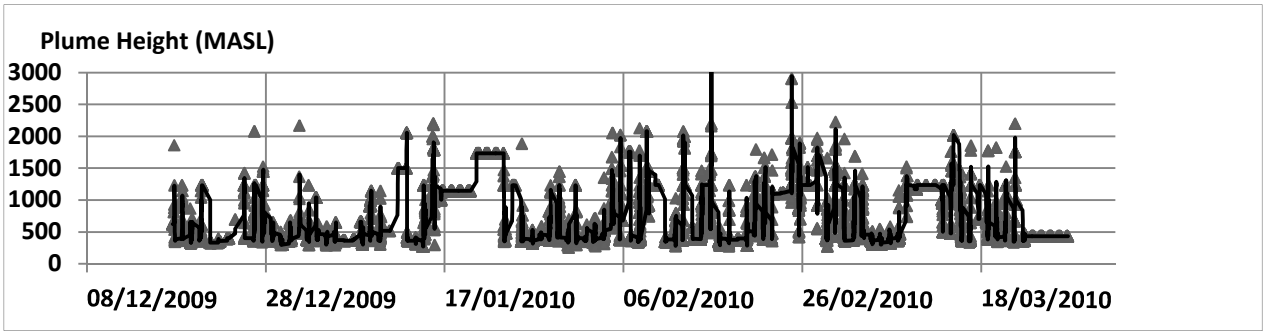

Figure 29. Plume height (MASL) during the measurement period. The height lies between 500 and 2000 mts. Some small degassing events can be noticed.

Wind speed information was obtained from the plume height estimations and the GDAS1 model of the National Ocean and Atmospheric Administration (NOAA). Although this model has a very low temporal-spatial resolution, it is the unique reference available to retrieve the wind speed. Other methods with a higher degree of accuracy are still in developing stages.

In Figure 28 we can observe a stable wind direction with a value of 270 ± 40˚ during the measurements period; in contrast, plume heights are varying during the day (Figure 29) with values that oscillate from 500 to 2000 masl. Clearly we cannot assume a constant plume height for flux retrieval; otherwise, the uncertainty in our measurements will be much higher. The results of our measurements are shown in Figure 30, also including daily seismic data reports from the Telica Seismic and Deformation Network

(TESAND) installed by The University of South Florida [Rodgers, Rodman; 2010]. During the measurement period the flux average was 115 t/d; but some individual measurements reported values as high as 2800 t/d. Previous measurements in 1997 reported 41 t/d; in November 1999 during an unusual increase of volcano activity, the values oscillated between 50 and 500 t/d [INETER 1997]. During a measurement campaign, using Mobile-DOAS, in November 2003; individual values of 249, 405, 493, 440, 1249 and 330 t/d were reported [Mather et all, 2005]. Our measurements are of the same order as the results reported in the campaign of November 2003. However; we have the advantage of a higher time resolution in our measurements compared to mobile transects; therefore, it is possible to estimate the variations of the flux emissions during the day. In a more detailed observation of the emission behavior during the whole measurement campaign, 3 different periods can be identified (Figure 30). Period 1 comprises the days between 17 December 2009 and 10 January 2010, as showing a varying daily flux with an average of 75 t/d. Period 2 comprises the days between 11 January 2010 and 21 January 2010, following a high peak increase in the SO_2 flux emission of 550 t/d. During this second period most of the days reported a flux value higher than 200 t/d. The average flux during this second period increased to 328 t/d; this is about 4 times higher compared to the flux average in period 1. Finally the period 3 comprises the days between 22 Janaury 2010 and 12 March 2010,when the fluxes varies similarly to period 1. The flux average in this period is 104 t/d; 40% higher compared to the average flux in period 1. The number of daily seismic events were compared individually in period 1, period 2 and period 3 with average values of 547, 712 and 633 respectively (Table 4.1). The variations in fluxes and the number of seismic events for each of these periods are in agreement according to their increase and decreases; although at different proportions. An agreement between flux increments and seismicity has been shown before at different volcanoes [Olmos et all, 2007 ; Edmonds et all,2003]
.

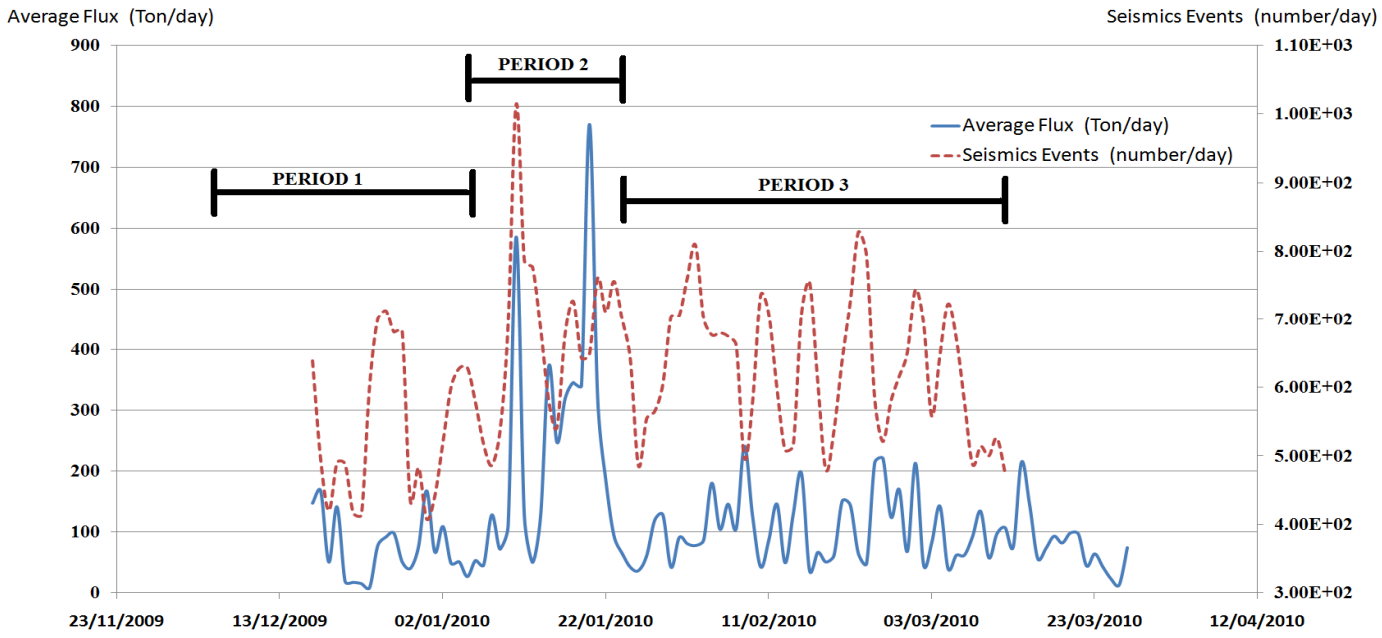

Figure 30. Daily SO_2 flux variations and daily amount of seismic events at Telica volcano from 17/12/2009 to 27/03/2010

Period	Average Flux	Average seismic Events
17/12/2009 - 10/01/2010	75	547
11/01/2010 - 21-01/2010	327	712
22/01/2010 – 12/03/2010	103	633

Table 4.1. Average flux and seismic events variation during the 3 identified periods

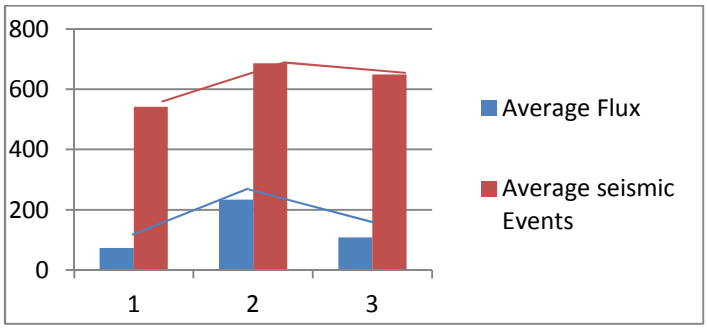

Figure 31. Flux average and seismic events average at the different periods

5.2 Popocatépetl Volcano

Several data sets were recorded during this field camping. The quick installing characteristic of the rapid deployment system allowed us to keep track of the spatial and temporal variations of the volcanic plume.

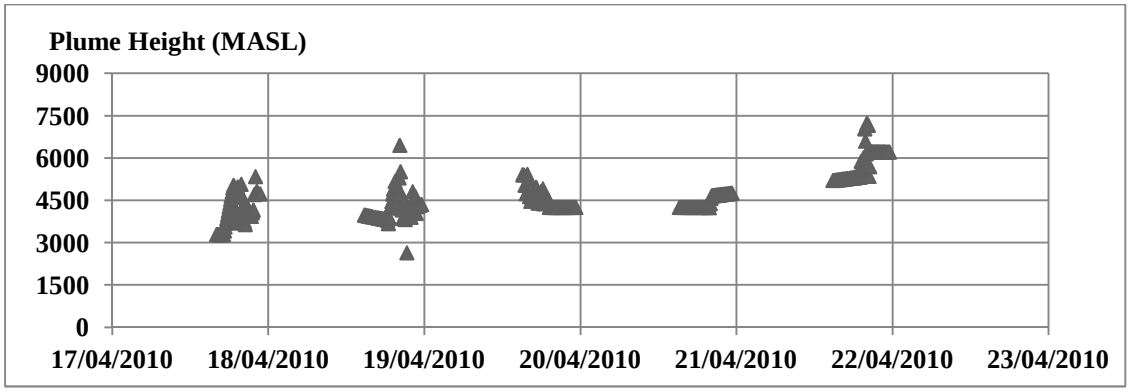

Figure 32. Plume height variations (masl) during the measurements conducted from 17/04/2010 to 21/04/2010.

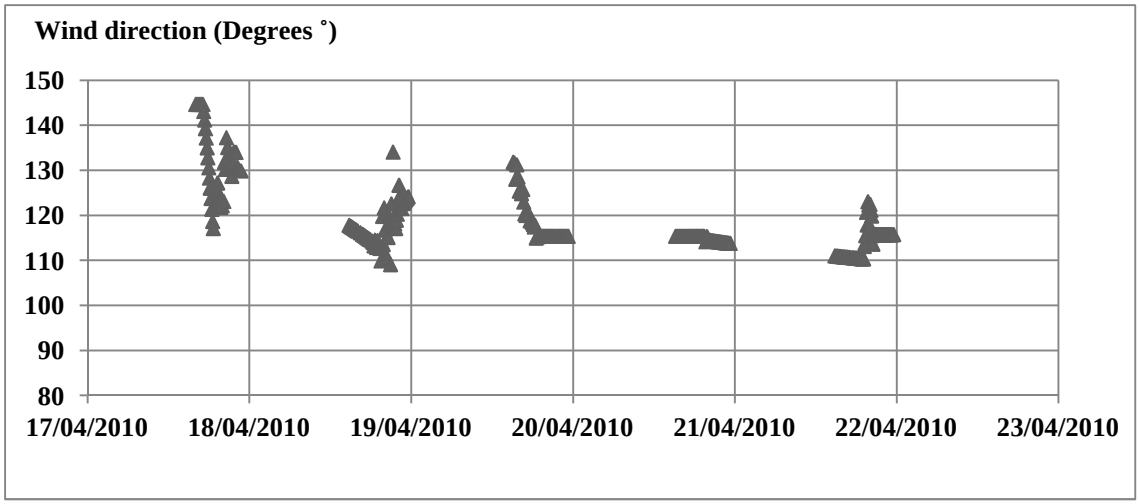

Figure 33. Wind direction (˚) during measurements during the period from 17/04/2010 to 21/04/2010.

Figure 32 and 33 show the temporal variation of plume height and wind direction. Since the volcanic edifice covers an area of about 78 Km^2, these small variations in the wind direction implied installing the instruments in different spots every day. In some cases there were different installation sites during the same day.

This constant tracking of the volcanic plume allowed us to get more accurate wind direction and plume height data; therefore improving the quality of our flux measurements. Wind speed data was obtained from the GDAS1 model of the National Ocean and Atmospheric Administration (NOAA). Accurate wind speed data is still very complicated to obtain and therefore is one of the major source of errors in flux measurements [Galle et al; 2010].

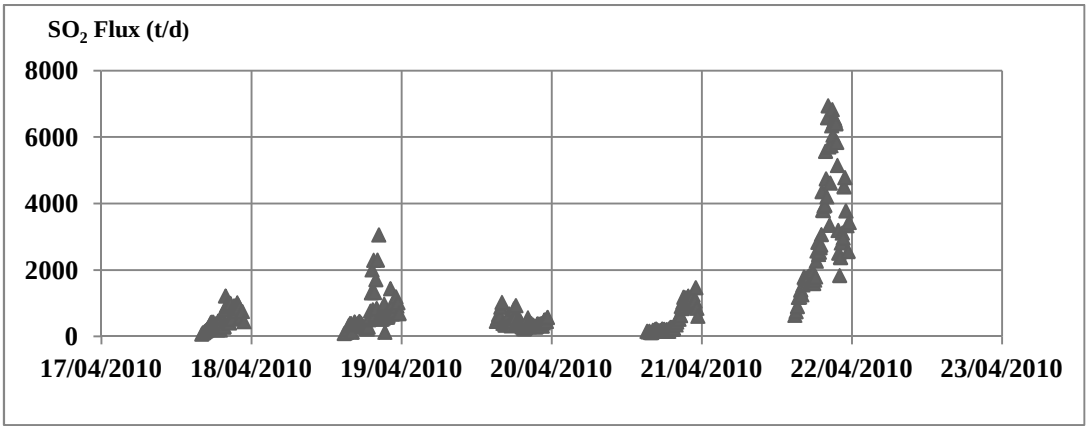

Figure 30. SO_2 flux (Ton/day) from 17/04/2010 to 21/04/2010.

The flux rate varies between 1000 and 1500 t/d in quiescent states. However some peaks were detected on 18 April 2010 and 21 April 2010. Small volcanic explosions are often reported in Popocatepelt volcano by the Centro Nacional para la Prevención de Desastres [CENAPRED]; thus, this is a possible explanation of the peaks in the flux measurements.

6 Conclusions

We had presented the details of design and field implementations of a rapid deployment system as a tool for monitoring gas emissions from volcanoes that is suitable for use during unexpected volcanic crisis even in areas of low accessibility.

The first test was on a field campaign on Telica volcano; from 17 December 2009 to 27 March 2010. The system worked unattended for a period of 3 months performing semi-continuous daylight measurements and transmitting the evaluated data via the BGAN satellite network. This setup shows the advantage of using high level computing resources for data processing in situ. A few years ago technological limitations were an impediment for developing autonomous systems capable of enduring outdoors conditions such as those presented in Nicaragua. The outcome of this field work provided a novel set of continuous measurement of SO_2 fluxes that allow to can be used to get a better understanding of future variations on Telica's eruptive activity. As a complement these gas emissions where compared with contemporaneous seismic activity records, thanks to their temporal resolution.

The second scenario of our application was a brief expedition to Popocatépetl volcano. On this occasion, the portability of the system was exploited in order to setup temporary installations following the daily natural variations of the volcanic plume due to the mainly variations in the wind regime.

Summarizing the results of the field experiments

Télica:

- The SO_2 flux emissions are around 118±104 t/d during our continuous measurement period of 3 months.
- The highest peak was preceded by an increase of the seismic events denoting a possible link.
- The wind direction tends to behave relatively stable, during the time of our measurements the predominant value was around 270 ± 40˚
- The measurements of the plume height reveal some variations around 500 masl and occasionally reaching up to 2000 masl. This peaking values can be attributed to some explosive events.

Popocatépetl:

- The mobility of the instrument allowed a continuos tracking of the volcanic plume despite the variations in the wind direction (110 -130˚).
- Flux rate of 1200±200 t/d in released states.
- The plume height observations showed that the plume lies between 5000 and 6500 masl. During explosive events the plume reached up to 7500 masl.

Although Scan-DOAS instruments are being used widely in many volcanoes in the world; it is important to remember that even if the system evaluates data automatically it is always necessary to consider possible sources of errors in the measurements in order to have reliable results; a task that requires of trained personal to control at the local observatories. High resolution meteorological weather data has always been challenging to obtain, like the wind speed, therefore this is one of the main sources of errors in our measurements. Other weather conditions like clouds and fog also affect the quality of the measurements. In addition, recent work has been conducted in order to characterize the radiative transfer errors in passive DOAS measurements [Christoph et all] that also increase the uncertainty of the data.

7 Acknowledgments

These instruments were founded by the Swedish international cooperation agency, SIDA and the NOVAC EU project. Special acknowledgments to the staff of INETER during the field campaign in Nicaragua. The field campaing in Mexico was founded by CONACYT and EU under the execution of the the project FIEL volcán. Special acknowledgments to the staff of CENAPRED-UNAM for their support during the field campaign in México.

8 References

Edmonds M, Herd R, Galle B, (2003). Automated hight time-resolution measurements of SO_2 flux at Soufrière Hillls Volcano, Montserrat.

Tralli D, Blom R, Zlotnicki V, Donnellan A, Evans D (2005). Satellite remote sensing of earthquake, volcano, flood, landslide and coastal inundation hazards. ISPRS 59: 185-198

Mc Gonilgle A, (2005) Volcano Remote Sensing with Ground-Based Spectroscopy. Phil. Trans. R. Soc 363, 2915-2929

Galle B, Oppenheimer C, Geyer A, McGonigle AJS, Edmonds M, Horrocks L (2003) A miniaturized ultraviolet spectrometer for remote sensing of SO2 fluxes: a new tool for volcano surveillance. J Volcanol Geotherm Res 119:241–254

Platt U, Stutz J (2008) Differential Optical Absorption Spectroscopy-principles and applications. Springer, Berlin Heidelberg New York

Mouginis-Mark P (2000) Remote sensing observations for volcano monitoring and hazard mitigation. ISPRS 33: B7

Tárraga M, Garcia A, Ortiz R, Abella R, Peña J (2001) SANARIS Project: A satellite network for natural risk monitoring. Natural Hazards 23: 417-429

Halmer, MM; Schmincke, H. 2004. The annual volcanic gas input into the atmosphere, in particular into the stratosphere: a global data set for the past 100 years.

Olmos R, Barrancos J, Rivera C, Barahona F, Lopez D, Henriquez B, Hernandez A, Benitez E, Hernandez P, Perez N, Galle B (2007) Anomalous Emissions of SO2 during the recent eruption of Santa Ana volcano, El Salvador, Central America. Pure and Applied Geophysics 164: 2489-2506

Bowman M (2008). Advanced Mobile Communications for Emergency Management and Crisis Response. Proceedings of The 2008 IAJC-IJME International Conference

Geoffrey W, Jhonson J, Ruiz M, Lees J, Welsh M (2005) Monitoring volcanic eruptions with a wireless sensor network. Second European workshop of wireless sensors networks

Christoph K, Deustschmann T, Vogel L, Wöhrbach M, Wagner T, Platt U (2009) Radiative transfer corrections for accurate spectroscopic measurements of volcanic gas emissions. Bull Volcanol 72: 233-247

Vandaele A, Simon P, Guilmot J, Carleer M, Colin R (1994) SO_2 absorption cross section measurements in the UV using a Fourier Transform Spectrometer. J. Geophys 99:25599-25605

Manat S, Lane A (1993) A compilation of the absorption cross-sections of SO_2 from 106 to 403 nm. Journal of Quantitative Spectroscopy and Radiative Transfer 50: 267-276

Kern C, Sihler H, Leif V, Rivera C, Herrera M, Platt U (2008) Halogen oxide measurements at Masaya Volcano, Nicaragua using active long path differential optical absorption spectroscopy Bulletin of volcanology 71: 659-670

Johansson M, Galle B, Zhang Y, Rivera C, Chen D, Wyser K (2009) The dual-beam mini-DOAS technique—measurements of volcanic gas emission, plume height and plume speed with a single instrument. Bulletin of volcanology 71: 747-751

http://bgansatellite.com/

http://www.freewave.com/

Instituto nicaraguense de estudios territoriales INETER: http://www.ineter.gob.ni

Centro nacional para la prevención de desastres CENAPRED: http://www.cenapred.unam.mx

NOVAC project: http://www.novac-project.eu/